

Asset Return & Camel Process: Beauty and the Beast [☆]

Zhenya Liu^{a,b}, Shixuan Wang^{b,*}

^a*Renmin University of China, Beijing, 100872, P.R. China*

^b*University of Birmingham, Birmingham, B15 2TT, UK*

Abstract

In this paper, we propose a new stochastic process named “camel process” for modelling the cumulative return of financial asset. This new process has three parameters, the market condition parameter α , the overreaction correction parameter β , and the volatility parameter γ . Its steady state probability density function (PDF) could be unimodal or bimodal, depending on the sign of the market condition parameter. The overreaction correction is realized through the non-linear drift term which incorporates the cube term of the instantaneous cumulative return. The time-dependent solution of its Fokker-Planck equation cannot be obtained analytically, but can be numerically solved by finite difference method. The properties of the camel process are confirmed by our empirical estimation results of ten market indexes in two different periods.

Keywords: Asset Return, Camel Process, Fokker-Planck Equation

JEL: C22, G12, G15

[☆]The research of Shixuan Wang was supported by the Economic and Social Research Council (UK) [grant number ES/J50001X/1] and a Royal Economics Society Junior Fellowship.

*Corresponding author

Email addresses: zhenya_liu@hotmail.com (Zhenya Liu), shixuan_wang@hotmail.com (Shixuan Wang)

1. Introduction

In this paper, we propose a new stochastic diffusion process called “camel process” to model the cumulative return of a financial asset. The beauty of the camel process is that it considers the market condition and the overreaction correction. The beast is that the time-dependent solution cannot be obtained analytically, but can be numerically solved by finite difference method. The name of the “camel process” is inspired by its property that the steady state probability density function (PDF) could be unimodal or bimodal, depending on the sign of the market condition parameter. The overreaction correction is realized through the non-linear drift term which incorporates the cube term of the instantaneous cumulative return.

There are two motivations for us to develop the camel process. Firstly, a financial market has two typical conditions, either sidewalk or trending¹. The behaviour of asset return is significantly different in the two market conditions. However, the asset return models in the existing literature seldom consider the market condition. Secondly, one drawback of the Geometric Brownian motion used in the derivation of the Black-Scholes model is that the price could go infinity, which is unrealistic. The camel process is designed to resolve those two problems.

We investigate the cumulative return rather than the price or log price for two reasons. First, overreaction can be easily measured by the cumulative return. Second, the cumulative return allows the comparison of investments in different financial assets. The cumulative return investigated by us is defined as

$$X_t = \sum_{t=1}^T r_t \quad (1)$$

where r_t is the log return ² of the price process $(P_t)_{t \geq 0}$ of the asset

$$r_t = \log(P_t) - \log(P_{t-1}) \quad (2)$$

The existing literature focuses on the improvement of the Black-Scholes from the perspective that explaining the stylized facts of asset returns. It is well documented that empirical daily return has stylized facts which are heavy-tail, “Long-Memory”, volatility clustering, Taylor effect, etc (see Granger & Ding, 1995; Pagan, 1996; Cont, 2001). Those stylized facts indicate that the independent normality assumption in the Black-Scholes model is unrealistic. In order to explain

¹A trending market includes both bull market and bear market.

²Like most researches, we prefer the log return rather than the arithmetic return $Y_t = (P_t - P_{t-1})/P_{t-1}$. The reason is that the cumulative return over n period is the sum of log return (shown in Equation 1), while the arithmetic return does not have this property.

the stylized facts, many researches have been devoted to modify the Geometric Brownian motion used in the derivation of the Black-Scholes model.

The first type of alternative models is to use fractional Brownian motions. Mandelbrot (1997) argues that successive price changes are not independent, and employs fractional Brownian motion to capture the dependent increments. In the finance study, a model should be self-consistent and shows no arbitrage opportunity (Kou, 2007). Nevertheless, Rogers (1997) proves that the fractional Brownian motion is not semi-martingale and shows the construction of arbitrage in the fractional Brownian motion.

Stochastic volatility and GARCH models are developed to capture the stylized fact of volatility clustering. Jäckel (2004) reviews various stochastic volatility models with focus on the dynamic replication of exotic derivatives and their implementation. Bollerslev et al. (1992) provides a comprehensive review on ARCH-family models. In addition to the price process, these models introduces another process for the evolution of volatility so that the time dependence of volatility could be captured.

Bingham & Kiesel (2001) asserts that the hyperbolic model is a good choice if someone wants a model that is more complex than the benchmark Black-Scholes model but less complicated than stochastic volatility models. Hyperbolic diffusion models are designed due to the empirical evidence that hyperbolic distributions could be fitted to daily returns with high accuracy (Eberlein & Keller, 1995). These models use hyperbolic distributions rather than normal distributions. Bibby & Sørensen (1996) model the logarithm of the stock price by an ergodic process with hyperbolic invariance measure, but their simulation shows that there is no significant difference between the option price inferred by the hyperbolic diffusion model and by the Black-Scholes model.

Merton (1976) derives an option pricing formula based on the assumption that the underlying stock returns are generated by the combination of continuous and jump processes. The unusual large practically returns can be explained by the jump-diffusion model, which can also replicate the heavy tail of the daily return distribution. Kou (2002) proposes a double exponential jump-diffusion model which gives analytical solutions for path-dependent options. Cont & Tankov (2004) reviews the models based on jump processes.

There are some other alternative models, “implied binomial tress” (Dupire et al., 1994), time changed Lévy process (Carr et al., 2003), and affine jump-diffusion models (Duffie et al., 2000).

2. The SDE and its properties

We propose a new stochastic process called ‘‘camel process’’ for the cumulative return of a financial asset. The camel process is defined as

Definition. The camel process solves the stochastic differential equation (SDE)

$$dX_t = (\alpha X_t - \beta X_t^3) dt + \gamma dW_t, \quad X_0 = 0 \quad (3)$$

where α , β , and γ are three parameters with $\alpha \in \mathbb{R}$, $\beta \in \mathbb{R}_{\geq 0}$, and $\gamma \in \mathbb{R}_+$.

Parameter α is named as market condition parameter. If $\alpha > 0$, the market is in a trending market condition. Otherwise, it is in a sidewalk market condition. Parameter β controls the correction for the overreaction behaviour in the market. If there is no overreaction occurred, β is essentially zero. Parameter γ measures the volatility of the process. In the camel process, the volatility is constant. In terms of the parameter space, α can be any real number, β is a non-negative real number, and γ can only take positive real number. Since the underlying process modelled is the cumulative return, the process always starts at zero.

2.1. Steady State PDF

It is difficult to analytically obtain the solution of the camel process due to its high order non-linear term. We here use the Fokker-Planck equation to make partial analytic analysis. For SDE, the Fokker-Planck equation is a partial differential equation (PDE) which describes the evolution of its probability density $p(X_t, t)$, namely the probability of realizations being near X_t at time t . The Fokker-Planck equation constructs a useful relationship between the solution of a SDE and its PDF along with time.

Applying the general Fokker-Planck equation on Equation 3 produces the PDF $p(X_t, t)$ for the camel process.

$$\frac{\partial p(X_t, t)}{\partial t} = -\frac{\partial}{\partial X_t} [(\alpha X_t - \beta X_t^3)p(X_t, t)] + \frac{\partial^2}{\partial X_t^2} \left[\frac{1}{2} \gamma^2 p(X_t, t) \right] \quad (4)$$

The steady state solution of the Fokker-Planck equation is the PDF evolving for a fairly long time so that it converges to a stable function which no longer change along with time t . The steady state PDF $p(X)$ of the camel process satisfies the time-independent Fokker-Planck equation by setting $\frac{\partial p(X_t, t)}{\partial t} = 0$.

$$0 = -\frac{\partial}{\partial X} [(\alpha X - \beta X^3)p(X)] + \frac{\partial^2}{\partial X^2} \left[\frac{1}{2} \gamma^2 p(X) \right] \quad (5)$$

Analytically solving ³ Equation 5 gives the solution of steady state PDF of the camel process

$$p(X) = A \exp\left(\frac{\alpha X^2 - \beta X^4/2}{\gamma^2}\right) \quad (6)$$

where A is the integration constant.

we show the steady-state PDF of the camel process could be unimodal or bimodal, depending on the sign of the market condition parameter α . Figure 1 displays the steady state PDF of the camel process for two combinations of parameter values. When α is less than zero, the steady state PDF is unimodal, which look like a one-humped camel. If α is larger than zero, the steady state PDF is bimodal, looking like a two-humped camel.⁴ The name of the ‘‘camel process’’ was inspired by the feature that its steady-state PDF could be unimodal or bimodal, which reminds people two types of camels.

Parameter α is named as market condition parameter since its sign determines whether the steady state PDF is unimodal or bimodal. The unimodal situation corresponds to the sidewalk market condition. In this situation, the underlying process (the cumulative return) has a tendency to zero because the SDE drift term has an opposite sign to its instantaneous cumulative return. Hence, the price series shows a mean-reverting pattern and the steady state PDF is centralized around zero. The bimodal situation corresponds to the trending market condition in which price tends to move towards upside or downside. In a trending market, a positive α generally causes that the SDE drift term has the same sign as the instantaneous cumulative return within the rational region. The cumulative return moves away from the start point, zero. In the steady state, the two modes of the PDF deviate from zero. The camel process is arbitrage-free and self-consistent. Either in unimodal situation or bimodal situation, the moving direction of the cumulative return is unknown. There is no arbitrage opportunity in our framework.

The price assumed by a Geometric Brownian motion can go up to infinity without any limit, which is not realistic. In order to resolve this problem, we use a non-linear drift term which incorporates the cube of the instantaneous cumulative return. Through this non-linear drift term, the underlying process cannot go to infinity. It will be corrected if it go beyond the rational level. Overreaction behaviour means that the price goes beyond its rational level. Correction on the overreaction means that we expect that the price would go back into its rational range if it is in the overreaction area. Note that overreaction only happens in the trending market condition.

³Details of mathematical derivation are presented in Appendix A.

⁴The case that α is equal to zero is shown in Appendix B.

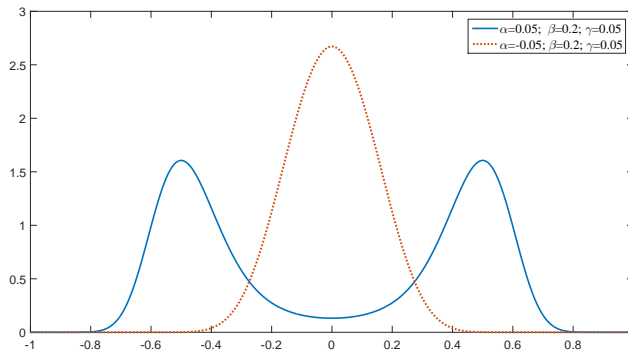


Figure 1: market condition Parameter α
Unimodal v.s. Bimodal

Parameter β is the parameter which controls the overreaction correction. Figure 2 displays the steady state PDF of both sidewalk and trending market condition. There is no big effect of the overreaction correction parameter β on the steady state PDF when the market is in sidewalk. However, the effect of β is vital if the market is in trending state. A larger value of β forces the mode of steady state PDF more close to zero. In contrast, the mode of steady state PDF can move further away if β is small.

The overreaction correction is realized through the non-linear drift term $\alpha X_t - \beta X_t^3$. Figure 3 shows the shape of the non-linear drift term under both market conditions. In a sidewalk market condition, the drift term always has the opposite sign as the instantaneous cumulative return. Hence, the cumulative return move towards to zero and shows the mean-reverting pattern. Under this situation, the overreaction correction normally rarely occurs. However, the overreaction correction plays a vital role in the trending market condition. As you can see in the lower panel of Figure 3, there is a middle region that the drift term has the same sign as the instantaneous cumulative return. There are other two side regions that the sign is opposite. The two side regions are deemed as the overreaction area. If the cumulative return go into the overreaction area, the drift term would force it move back the rational region, which is the one in the middle.

The range of the rational region is control by the parameter β . If the value of β is large, then the magnitude of overreaction correction is stronger and the rational region is narrower. Conversely, a smaller β means that the market can tolerate overreaction to a larger extent. Thus, the range of the rational region is wider.

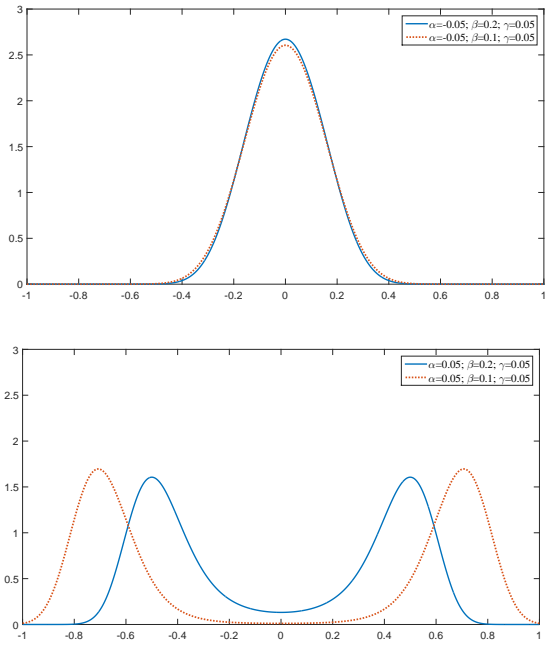


Figure 2: Volatility Parameter β

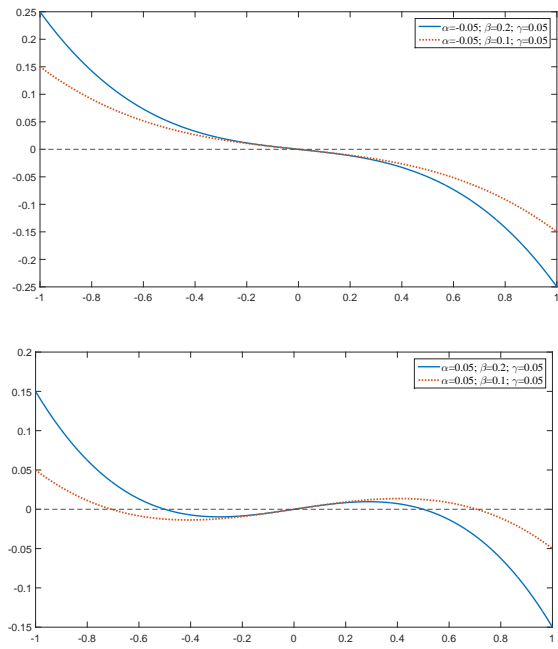


Figure 3: Drift Term

Parameter γ is named as the volatility parameter. It controls the volatility magnitude of the dW_t . Figure 4 illustrates that the steady state PDF is more diversified with a larger value of γ . By contrast, a smaller value of γ results in a more centralized steady state PDF. Importantly, the mode of the steady state PDF remains the same regardless the change of the value of γ under both unimodal or bimodal situations. The mode of the steady state PDF only depends on the market condition parameter α and the overreaction parameter β .

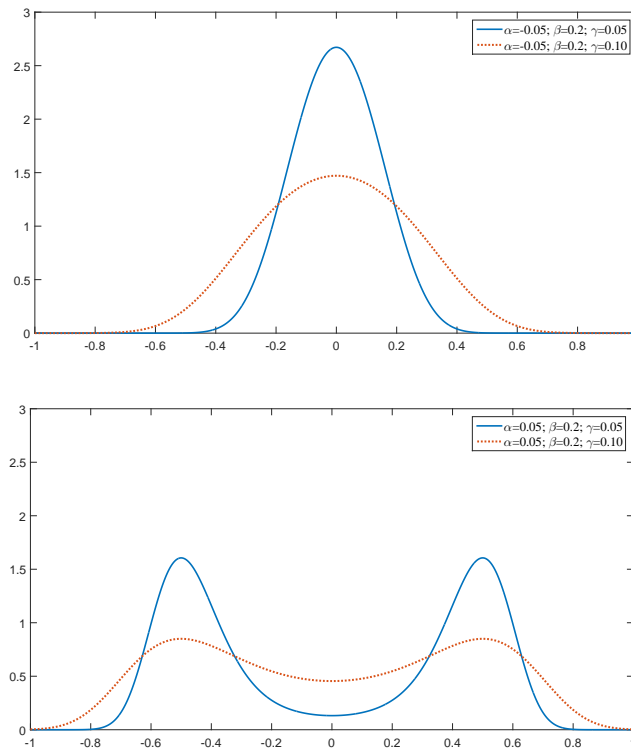


Figure 4: Volatility Parameter γ

2.1.1. Time Dependent PDF

Without the assumption $\frac{\partial p(X_t, t)}{\partial t} = 0$, the solution of Equation 4 is the time dependent PDF $p(X_t, t)$ of the camel process, which is evolving with time t and converges to its steady state PDF $p(X)$. The analytical solution of the Fokker-Planck equation can only be obtained in a limited special cases, and mostly in the steady state (Pichler et al., 2013). During the past five decades, a number of numerical methods have been developed to obtain the approximated solution of the Fokker-Planck equation. These numerical methods includes weighted residual method,

eigenfunction expansion, finite differences, and finite elements. Here, we follow Roberts (1986) to use the finite difference method to solve the Fokker-Planck equation for the one-dimensional⁵ time dependent PDF. Although there are more accurate higher order finite difference schemes (see Wojtkiewicz et al., 1997), Roberts' method is enough for the one-dimensional Fokker-Planck equation. Our examples show the numerically solved time dependent PDF converges to steady state PDF accurately.

In order to use finite difference method to numerically solve the Fokker-Planck equation, we need to clarify the initial condition, the boundary condition, and the normalization condition. The initial condition $p(X_0, 0)$ is given by the Dirac delta function

$$p(X_0, 0) = \delta(X_0 - 0) \quad (7)$$

where X_0 is zero since the underlying process is the cumulative return.

The boundary condition is imposed by a zero-flux condition at infinity of X_t

$$p(X_t, t) \rightarrow 0 \quad \text{as} \quad X_t \rightarrow \pm\infty \quad (8)$$

Additionally, the normalization condition for the time dependent PDF is given by

$$\int p(X_t, t) dX_t = 1 \quad (9)$$

Here, we derive the explicit scheme of the Finite Difference method. Applying the chain rule on Equation 4, we can obtain

$$\frac{\partial p(X_t, t)}{\partial t} = (-\alpha + 3\beta X_t^2)p(X_t, t) + (-\alpha X_t + \beta X_t^3) \frac{\partial p(X_t, t)}{\partial X_t} + \frac{1}{2}\gamma^2 \frac{\partial^2 p(X_t, t)}{\partial X_t^2} \quad (10)$$

In order to keep the notation cleaner, we suppress the time subscript of X_t as X , and suppress the argument X_t and t of the time dependent PDF $p(X_t, t)$ and use the notation p .

$$\frac{\partial p}{\partial t} = (-\alpha + 3\beta X^2)p + (-\alpha X + \beta X^3) \frac{\partial p}{\partial X} + \frac{1}{2}\gamma^2 \frac{\partial^2 p}{\partial X^2} \quad (11)$$

In terms of central finite differences, the above PDF becomes

$$\frac{p_i^{m+1} - p_i^m}{\Delta t} = (-\alpha + 3\beta X^2)p_i^m + (-\alpha X + \beta X^3) \frac{p_{i+1}^m - p_{i-1}^m}{2\Delta X} + \frac{1}{2}\gamma^2 \frac{p_{i+1}^m - 2p_i^m + p_{i-1}^m}{\Delta X^2} \quad (12)$$

where m is the integer index of the mesh on time and i is the integer index of the mesh on the space.

⁵In our case, there is only spatial variable X_t besides the time variable t .

The explicit scheme is obtained for the time dependent PDF

$$p_i^{m+1} = p_i^m + \Delta t \left\{ (-\alpha + 3\beta X^2)p_i^m + (-\alpha X + \beta X^3) \frac{p_{i+1}^m - p_{i-1}^m}{2\Delta X} + \frac{1}{2}\gamma^2 \frac{p_{i+1}^m - 2p_i^m + p_{i-1}^m}{\Delta X^2} \right\} \quad (13)$$

Using this scheme, the values p_i^{m+1} can be calculated directly from values p_i^m . Under the initial condition, boundary condition, and the normalization condition, the time dependent PDF can be solved directly.

Figure 5 displays two examples of the numerical solution of the time dependent PDF starting at time 1 ⁶. The upper panel is the case of sidewalk market condition which α is negative. The Lower panel is the case of trending market condition which α is positive. In the sidewalk market condition, the time dependent PDF is always unimodal. While in the trending market condition, the time dependent PDF at the early stage is unimodal because it evolves from the initial condition which is a Dirac delta function. After some periods, the time dependent PDF appears to be bimodal and the density around the two modes is getting increasingly higher along with time.

Figure 6 shows some slices of the time dependent PDF and compares them with the steady state PDF. In the upper panel (sidewalk market condition), the time dependent PDF converges to the steady state PDF quickly. The difference is subtle between time dependent PDF at $t = 20$ and steady state. After 50 periods, the time dependent PDF almost overlaps with the steady state PDF. However, the convergence rate in the lower panel (trending market condition) is slower. At $t = 20$, the time dependent PDF is still unimodal. After 40 periods, we can observe that the time dependent PDF is bimodal and evolves towards the steady state PDF. At $t = 100$, it is not obvious to distinguish the time dependent PDF and the steady state PDF.

⁶The PDF at time 0 is omitted here because that is the initial condition which is a Dirac delta function.

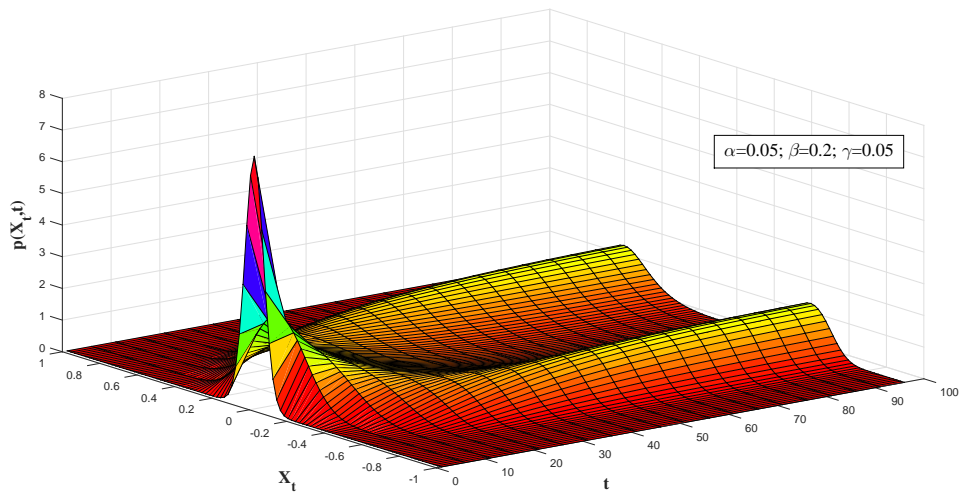
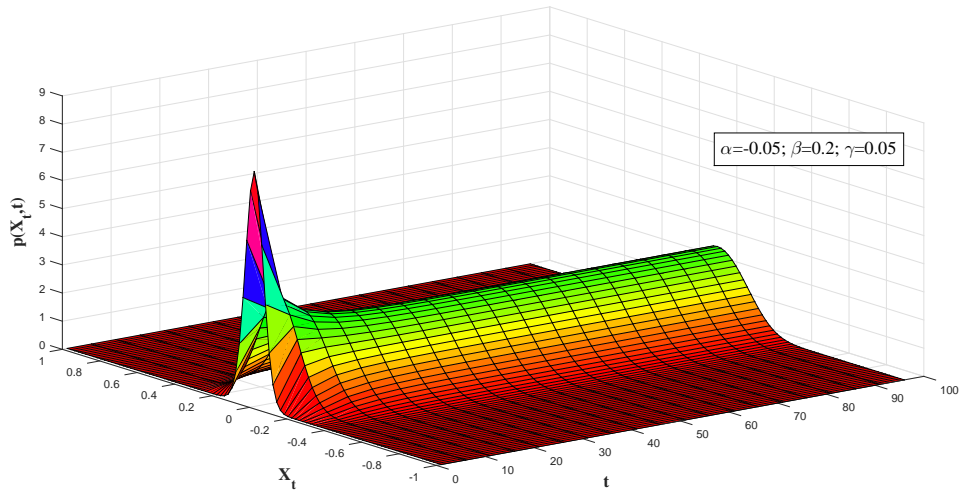


Figure 5: Time Dependent PDF

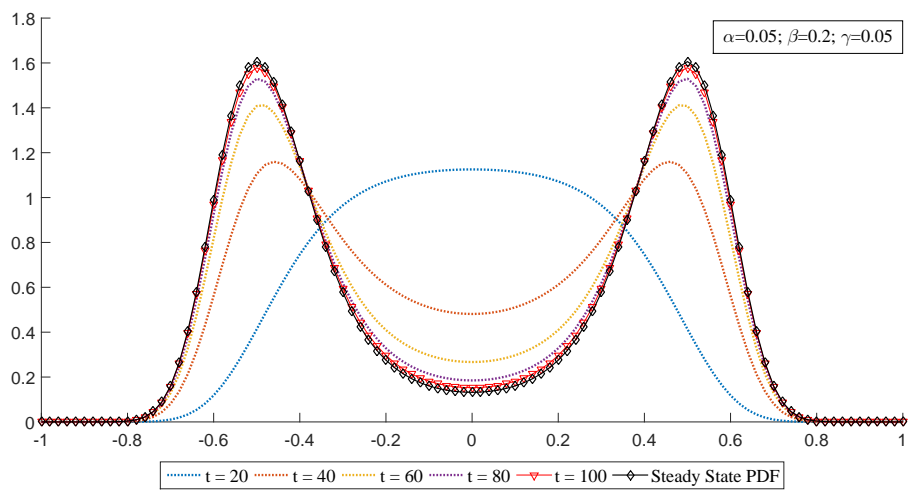
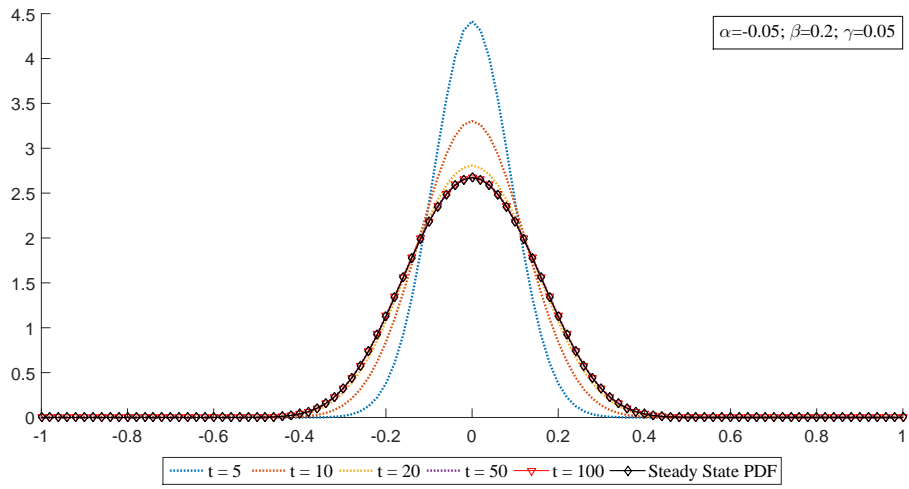


Figure 6: Time Dependent PDF Slices v.s. Steady State PDF

3. Empirical Study

3.1. Data

The maximum likelihood method is employed to estimate the camel process for ten stock market indexes, S&P 500, FTSE 100, CAC 40, DAX, Nikkei 225, STI, ASX 200, CSI 300 (a.k.a. SHSE 300), HSI, and TAIEX. We download daily closing prices from Yahoo Finance and compute the cumulative returns by Equation 1. We are particularly interested in two specific periods, August 1st 2008 to March 31st 2009 and May 1st 2014 to April 30th 2016. The first period is after the financial crisis in 2008 and all markets experienced a downside trend. Thus, we expect to see the estimated market condition parameters $\hat{\alpha}$ are all positive for different markets. The second period is the recent year and different markets may behave differently. We can use the estimated parameters to investigate their market conditions and magnitude of overreaction correction for the two periods.

3.2. Maximum Likelihood Estimator

The log likelihood function for the camel process given a specific dataset is

$$\mathcal{L}(\Theta) = \sum_{t=1}^T \log p(X_t, t | \Theta) \quad (14)$$

where $\Theta = \{\alpha, \beta, \gamma\}$, X_t is the observation at time t , and $p(X_t, t | \Theta)$ is the numerical solver of Equation 10. The maximum likelihood method estimates parameters by maximizing the log likelihood function.

$$\hat{\Theta} = \arg \max_{\Theta} \sum_{t=1}^T \log p(X_t, t | \Theta) \quad (15)$$

where $\hat{\Theta}$ needs to stay in the parameter space that $\alpha \in \mathbb{R}$, $\beta \in \mathbb{R}_{\geq 0}$, and $\gamma \in \mathbb{R}_+$.

3.3. Estimation Result

Table 1 presents the estimated parameters for ten indexes during two periods. In the first period (Aug. 2008 to Apr. 2009), the estimated market condition parameter $\hat{\alpha}$ are all positive, indicating that they were all in a trending market condition. This is consistent with the reality that all ten markets had a downside trend after the financial crisis. S&P 500, STI and DAX have relatively large values of $\hat{\beta}$, implying that those three markets had strong overreaction correction for the market crash after the financial crisis.

Table 1: Estimation Result

	Aug. 2008 ~ Apr. 2009				May. 2015 ~ Apr. 2016			
	$\hat{\alpha}$	$\hat{\beta}$	$\hat{\gamma}$	likelihood	$\hat{\alpha}$	$\hat{\beta}$	$\hat{\gamma}$	likelihood
S&P500	0.498	4.217	0.256	98.513	-0.106	0.000	0.025	536.050
FTSE100	0.057	0.680	0.039	193.790	0.010	0.515	0.011	480.400
CAC40	0.070	0.551	0.056	138.760	-0.020	0.666	0.024	436.110
DAX	0.237	1.790	0.113	110.950	0.009	0.568	0.011	439.200
Nikkei225	0.084	0.374	0.034	165.020	-0.039	1.418	0.036	394.420
STI	0.063	2.592	0.349	22.264	0.021	0.351	0.019	357.100
ASX200	0.046	0.407	0.027	223.150	0.020	0.883	0.008	529.300
CSI300	0.092	0.657	0.059	131.820	0.208	1.748	0.109	182.570
HSI	0.085	0.308	0.056	137.570	0.069	0.845	0.041	269.690
TAIEX	0.246	1.624	0.093	123.190	0.016	0.521	0.012	420.130

In the second period (May. 2015 to Apr. 2016), S&P, CAC 40 and Nikkei 225 were in a sidewalk condition, while other markets were in a trending condition. CSI 300 has highest value of the estimated market condition parameter $\hat{\alpha}$ (0.208), suggesting that the Chinese market experienced a relatively large trend. Our estimation result is consistent with reality. Figure 7 compares the cumulative return of S&P 500 and CSI 300. It is clear that S&P 500 was in a sidewalk market condition in which its cumulative return was fluctuating around zero, while CSI 300 had a big trend and its cumulative return largely deviated from zero.

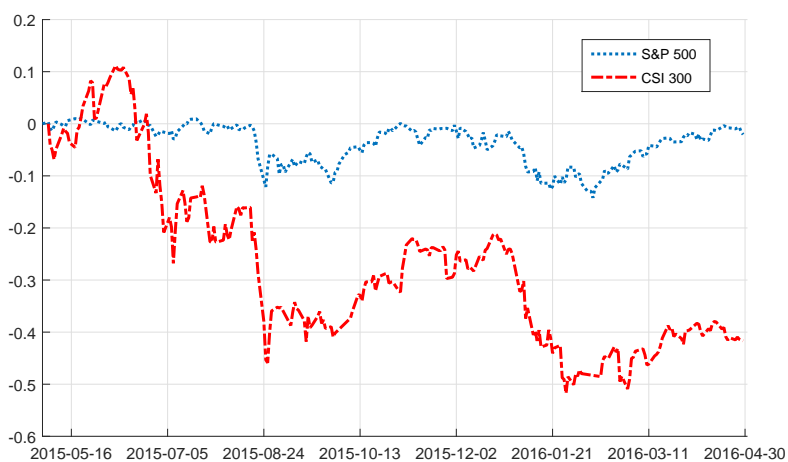


Figure 7: Cumulative Return of S&P 500 and CSI 300 (May. 2015 to Apr. 2016)

4. Conclusion

In this paper, we propose a new stochastic process named “camel process” for modelling the cumulative return of financial asset. This new process has three parameters, the market condition parameter α , the overreaction correction parameter β , and the volatility parameter γ . Its steady state probability density function (PDF) could be unimodal or bimodal, depending on the sign of the market condition parameter. The overreaction correction is realized through the non-linear drift term which incorporates the cube term of the instantaneous cumulative return. The time-dependent solution of its Fokker-Planck equation cannot be obtained analytically, but can be numerically solved by finite difference method. The properties of the camel process are confirmed by our empirical estimation results of ten market indexes in two different periods. A limitation of this paper is that the parameters of the camel process is possibly time-varying. Future research may wish to develop the change point detection for the camel process.

Appendix A. Steady State Solution of the Fokker-Planck Equation

Theorem (Fokker-Planck equation). *Consider the Ito process X_t with drift $\mu(X_t)$ and volatility $\sigma(X_t)$, and hence satisfying the SDE $dX_t = \mu(x_t)dt + \sigma(x_t)dW_t$. The probability density function (PDF) of the ensemble of realizations $p(X_t, t)$ satisfies the Fokker-Planck equation ⁷.*

$$\frac{\partial p(X_t, t)}{\partial t} = -\frac{\partial}{\partial X_t} [\mu(X_t)p(X_t, t)] + \frac{\partial^2}{\partial X_t^2} \left[\frac{1}{2} \sigma(X_t)^2 p(X_t, t) \right]$$

The camel process solves the SDE

$$dX_t = (\alpha X_t - \beta X_t^3)dt + \gamma dW_t, \quad X_0 = 0 \tag{A.1}$$

where $\alpha \in \mathbb{R}$, $\beta \in \mathbb{R}_{\geq 0}$, and $\gamma \in \mathbb{R}_+$. The drift term is $\alpha X_t - \beta X_t^3$ and the volatility term is γ .

The Fokker-Planck equation for the camel process is

$$\frac{\partial p(X_t, t)}{\partial t} = -\frac{\partial}{\partial X_t} [(\alpha X_t - \beta X_t^3)p(X_t, t)] + \frac{\partial^2}{\partial X_t^2} \left[\frac{1}{2} \gamma^2 p(X_t, t) \right] \tag{A.2}$$

By setting $\frac{\partial p(X_t, t)}{\partial t} = 0$, we can obtain the steady state PDF $p(X)$ which satisfies the time-independent Fokker-Planck equation

$$0 = -\frac{\partial}{\partial X} [(\alpha X - \beta X^3)p(X)] + \frac{\partial^2}{\partial X^2} \left[\frac{1}{2} \gamma^2 p(X) \right] \tag{A.3}$$

⁷The Fokker-Planck equation is also known as the Kolmogorov forward equation.

One integral with respect to X

$$\begin{aligned}\int 0 \, dX &= \int -\frac{\partial}{\partial X} [(\alpha X - \beta X^3)p(X)] + \frac{\partial^2}{\partial X^2} \left[\frac{1}{2} \gamma^2 p(X) \right] dX \\ 0 &= -(\alpha X - \beta X^3)p(X) + \frac{\partial}{\partial X} \left[\frac{1}{2} \gamma^2 p(X) \right] + \text{constant} \\ \text{constant} &= -(\alpha X - \beta X^3)p(X) + \frac{\partial}{\partial X} \left[\frac{1}{2} \gamma^2 p(X) \right]\end{aligned}$$

This constant must be zero, as $p(X)$ and its derivatives have to vanish for large enough X

$$\begin{aligned}0 &= -(\alpha X - \beta X^3)p(X) + \frac{\partial}{\partial X} \left[\frac{1}{2} \gamma^2 p(X) \right] \\ 0 &= -(\alpha X - \beta X^3)p(X) + \frac{1}{2} \gamma^2 \frac{dp(X)}{dX} \\ \frac{1}{2} \gamma^2 \frac{dp(X)}{dX} &= (\alpha X - \beta X^3)p(X) \\ \frac{1}{p(X)} dp(X) &= \frac{2(\alpha X - \beta X^3)}{\gamma^2} dX\end{aligned}$$

Integral on both hand sides

$$\begin{aligned}\int \frac{1}{p(X)} dp(X) &= \int \frac{2(\alpha X - \beta X^3)}{\gamma^2} dX \\ \log p(X) &= \int \frac{2\alpha X}{\gamma^2} - \frac{2\beta X^3}{\gamma^2} dX \\ &= \int \frac{2\alpha X}{\gamma^2} dX - \int \frac{2\beta X^3}{\gamma^2} dX \\ &= \frac{\alpha X^2}{\gamma^2} - \frac{\beta X^4/2}{\gamma^2} + \text{constant} \\ &= \frac{\alpha X^2 - \beta X^4/2}{\gamma^2} + \text{constant}\end{aligned}$$

Taking exponential on both hand sides produce the solution

$$p(X) = A \exp \left(\frac{\alpha X^2 - \beta X^4/2}{\gamma^2} \right) \quad (\text{A.4})$$

where A is the integration constant. In order to determine the integration constant A , we can use the property of PDF that the area underneath must be one.

$$\begin{aligned}1 &= \int_0^\infty A \exp \left(\frac{\alpha X^2 - \beta X^4/2}{\gamma^2} \right) dX \\ 1 &= A \int_0^\infty \exp \left(\frac{\alpha X^2 - \beta X^4/2}{\gamma^2} \right) dX \\ A &= \left(\int_0^\infty \exp \left(\frac{\alpha X^2 - \beta X^4/2}{\gamma^2} \right) dX \right)^{-1}\end{aligned}$$

Applying series expansion and integrating with respect to individual items

$$A = \left(\frac{1}{2} \sum_{m=0}^{\infty} \frac{\left(\frac{\alpha}{\gamma^2}\right)^m}{m!} \frac{\Gamma\left(\frac{2m+1}{4}\right)}{\left(\frac{\beta}{2\gamma^2}\right)^{\frac{2m+1}{4}}} \right)^{-1} \quad (\text{A.5})$$

where $\Gamma(\cdot)$ is the gamma function.

Appendix B. Steady State PDF when α is zero

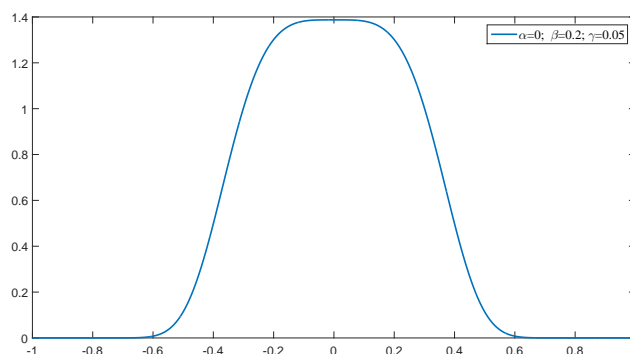


Figure B.8: when α is zero, the Steady State PDF has a flat area near zero in the x-axis.

References

- Bibby, B. M., & Sørensen, M. (1996). A hyperbolic diffusion model for stock prices. *Finance and Stochastics*, 1, 25–41.
- Bingham, N. H., & Kiesel, R. (2001). Modelling asset returns with hyperbolic distributions. *Return Distributions in Finance*, (pp. 1–20).
- Bollerslev, T., Chou, R. Y., & Kroner, K. F. (1992). Arch modeling in finance: A review of the theory and empirical evidence. *Journal of econometrics*, 52, 5–59.
- Carr, P., Geman, H., Madan, D. B., & Yor, M. (2003). Stochastic volatility for lévy processes. *Mathematical Finance*, 13, 345–382.
- Cont, R. (2001). Empirical properties of asset returns: stylized facts and statistical issues. *Quantitative Finance*, 1:2, 223–236.

- Cont, R., & Tankov, P. (2004). *Financial modelling with jump processes*. Chapman & Hall.
- Duffie, D., Pan, J., & Singleton, K. (2000). Transform analysis and asset pricing for affine jump-diffusions. *Econometrica*, *68*, 1343–1376.
- Dupire, B. et al. (1994). Pricing with a smile. *Risk*, *7*, 18–20.
- Eberlein, E., & Keller, U. (1995). Hyperbolic distributions in finance. *Bernoulli*, (pp. 281–299).
- Granger, C. W., & Ding, Z. (1995). Some properties of absolute return: An alternative measure of risk. *Annales d'Economie et de Statistique*, (pp. 67–91).
- Jäckel, P. (2004). *Stochastic volatility models: past, present and future*. Chichester, UK: Wiley.
- Kou, S. (2007). Jump-diffusion models for asset pricing in financial engineering. *Handbooks in operations research and management science*, *15*, 73–116.
- Kou, S. G. (2002). A jump-diffusion model for option pricing. *Management science*, *48*, 1086–1101.
- Mandelbrot, B. B. (1997). *The variation of certain speculative prices*. Springer.
- Merton, R. C. (1976). Option pricing when underlying stock returns are discontinuous. *Journal of financial economics*, *3*, 125–144.
- Pagan, A. (1996). The econometrics of financial markets. *Journal of empirical finance*, *3*, 15–102.
- Pichler, L., Masud, A., & Bergman, L. (2013). Numerical solution of the fokker–planck equation by finite difference and finite element methods a comparative study. In *Computational Methods in Stochastic Dynamics* (pp. 69–85). Springer.
- Roberts, J. (1986). First-passage time for randomly excited non-linear oscillators. *Journal of Sound and vibration*, *109*, 33–50.
- Rogers, L. C. G. (1997). Arbitrage with fractional brownian motion. *Mathematical Finance*, *7*, 95–105.
- Wojtkiewicz, S., Bergman, L., & Spencer Jr, B. (1997). High fidelity numerical solutions of the fokker-planck equation. In *Proceedings of the ICOSSAR 97, The Seventh International Conference on Structural Safety and Reliability, Kyoto, Japan, Nov* (pp. 24–28).